Computational Structural Engineering
An International Journal
Vol. 1, No. 1, pp. 1~9 (2001)

Computational Structural Engineering Institute

Post-earthquake Assessment of Mission-Gothic Undercrossing

K.Y. Lou[1], J.F. Ger[2], R.J. Yang[3], and F.Y. Cheng[†]

[1]Dept. of Civ. Engrg., Senior Investigator, Intelligent systems Center, Univ. of Missouri-Rolla, 301A Butler-Carlton civil Engrg. Hall Univ. of MO-Rolla, Rolla, MO 65409-0030, USA
[2]Martin and Huang International, Inc., 48 South Chester Ave., Pasadena, CA 91106, USA Bridge Division, Missouri Department of Transportation, P.O. Box 270, Jefferson City, MO 65102, USA
[3]Structural Engineer, Ph.D., Carson K.C. Mok Consulting Engineering, P.A., 9001 Ottawa Place, Silver Spring, MD, 20910, USA

Received November 2000; Accepted April 2001

ABSTRACT

Collapse behavior of Mission-Gothic Undercrossing under Northridge earthquake is studied by performing nonlinear time-history analysis and three-dimensional nonlinear finite element method for flared columns. Bridge structural model is characterized as three-dimensional with consideration of columns, superstructures, and abutment conditions. Three components of ground motion, corresponding to bridge's longitudinal, transverse, and vertical direction and their combinations are used to investigate bridge collapse. Studies indicate that bridge collapse is dominantly caused by transverse ground motion and the consideration of three-dimensional ground motion leads to a more accurate assessment. Failure mechanism of flared columns is analyzed applying nonlinear finite element method. Reduction of column capacity is observed due to orientation of flare. Further investigation demonstrates that the effects of flare play an important role in predicting of bridge failure mechanism. Suggestions are offered to improve the performance of bridges during severe earthquake.

Keywords: bridge structures, columns, dynamic analysis, finite element, flare, ground motion, nonlinearity, Northridge earthquake, reinforced concrete, shear key failure, stiffness, yielding.

1. Introduction

Mission-Gothic Undercrossing, located on State Route 118 San Fernando Freeway, collapsed during the January 17, 1994 Northridge earthquake. It features a skew layout of abutments and bents, directional dependence of flared column stiffness, and no stirrups to enclose flare reinforcement in the lower part of the flare (see Figs. 1 and 2). Field observation after the earthquake indicates that the bridge collapse mainly resulted from these characteristics. However, the dominant cause and the subsequence of these characteristics to bridge collapse remain unclear and need further studies. It is because that systematic investigation will give deep insight into seismic performance of reinforced concrete bridges, which were built in the same age as Mission-Gothic Undercrossing.

Studies of collapse behavior focus on nonlinear time-history analysis of three-dimensional structural systems. Superstructures of bridges are treated as linear elements, while columns are modeled as inelastic ones. Yielding surface of column segments under the interaction of longitudinal load and biaxial bending is first developed for structural system analysis. Abutment conditions are also taken into account. Ground motion recorded at Sylmar

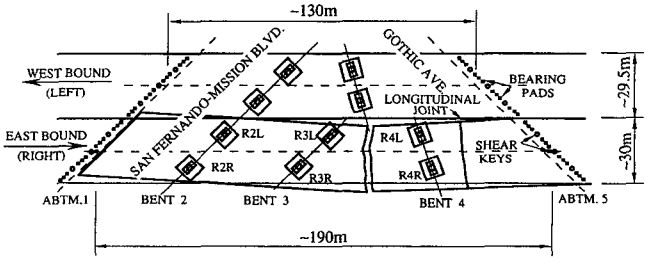

Fig. 1. Layout of Mission-Gothic Undercrossing.

[†] Corresponding author
Tel.: 573-341-4469; Fax: 573-341-4729
E-mail address: fycheng@umr.edu

County Hospital parking lot, which was about 18 km away from the epicenter, is modified to consider the distance effect between the recording station and the bridge.

To investigate the performance of flared columns of Mission-Gothic Undercrossing Bridge, an algorithm of nonlinear finite element analysis (Lou and Cheng, 1994) is developed and applied. Different combinations of ground motion are chosen to compare structural response, unfavorable internal forces in columns and the like, and thus demonstrate the role of vertical ground motion on bridge failure. Effects of the flare on a structural model are also investigated to evaluate the role of these architectural elements in bridge failure mechanism. Suggestions based on analysis are proposed to improve the performance of bridges under severe earthquake.

2. Bridge Collapse Description

Mission-Gothic Undercrossing is composed of two parallel bridge structures over the intersection of San Fernando-Mission Boulevard and Gothic Avenue in Los Angeles. It was designed in 1973 and built in 1976. The two-bridge structure right and left are separated by a longitudinal joint seal. The right bridge is approximately 190 m (622 ft) long and 30 m (98.25 ft) wide with four spans. The left one is a three-span bridge approximately 130 m (427 ft) in length and 20.5 m (96.75 ft) in width. Both are supported on two-column bents and abutments. Fig. 1 shows the layout of the bridge.

Bridge abutments were designed to be parallel to San Fernando-Mission Boulevard and Gothic Avenue. Therefore, a significant difference in length of the two structures results from skew abutments. Abutment 1, bent 2, and bent 3 of right structure skew approximately 45° clockwise, while bent 4 and abutment 5 skew approximately 11° and 45° counterclockwise, respectively.

The superstructure is a multi-cell, cast-in-place post-tensioned box girder with a structural depth of 2.29 m (7.5 ft), sitting on twelve 457 mm × 457 mm × 76 mm (18 in. × 18 in. × 3 in.) elastomeric bearing pads at abutments. Each bridge end consists of three 762 mm (30 in.) square shear keys, which are embedded 381 mm (15 in.) into the abutment seat, allowing the superstructure to be able to move 152 mm (6 in.) in the bridge's longitudinal direction.

Column height varies from 6.77 m (22.2 ft) to 7.53 m (24.7 ft), measuring from the bottom soffit to the top of the footing. At each bent, the lower part of column is octagonal and 1.829 m (6 ft) in diameter with 45 #35 longitudinal reinforcement, and is confined by #15 spiral with 90 mm (3.5 in.) pitch. A one-way flare in the bent direction is over a 3.66 m (12 ft) transitional length, and ends at the bottom soffit with a 1.829 m × 4.267 m (6 ft × 14 ft) rectangular cross-section. Twenty-two #35 flare reinforcement starts at the bottom of the flare and extends 1.829 m (6 ft) into the cap beam. Across the top 2.44 m (8 ft) of the flare are rectangular stirrups #15 at a spacing of 305 mm (12 in.). But there is no stirrup to enclose flare reinforcement along the lower part comprising 1.22 m (4 ft) of the flare. Reinforcement details of the column are shown in Fig. 2a.

Footings are placed on 406 mm (16 in.) diameter 70-ton concrete piles. Dimensions of footing change from 6.10 m (20 ft) to 7.32 m (24 ft) in both directions and vary between 1.52 m (5 ft) and 1.98 m (6.5 ft) in depth.

As shown in Fig. 1, the right bridge structure collapsed completely between span 3 and 4 ("The Northridge" 1994; "Preliminary" 1994). Span 1 and 2 did not fail completely but incurred severe damage. Abutment 1 remained seated with very little longitudinal movement. Approximately 330 mm (13 in.) of transverse movement was observed. At bent 2, the right column failed and slid on the footing surface due to damage of the reinforced concrete collar, and the left column collapsed, dropping its flare to the side of the column. Columns at bent 3 failed and displayed heavy spalling over the flare, while bent 4 completely collapsed (Priestley *et al.*, 1994). At abutment 5, the end diaphragm was unseated. The left bridge structure did not collapse although it suffered severe damage. Most columns were damaged in the flare region (see Fig. 2b), but remained standing ("The Northridge" 1994). The end diaphragm was seated. Fifty-one mm (2 in.) of transverse displacement and 76 mm (3 in.) of longitudinal movement were measured at abutment 1. At abutment 5, transverse movement of 254 mm (10 in.) was observed.

3. Nonlinear Finite Element Analysis of Flared Column

3.1 Nonlinear Finite Element Model

Flare in the upper part of columns was originally designed by Caltrans for reasons of architectural aesthetics ("The Northridge" 1994). Flare design philosophy involved sufficient longitudinal reinforcement and inadequate stirrups. Reinforcement details of the flare were not intended to increase column strength. Flare is expected to fail after an earthquake, but can be repaired. However, damage to the flare from field observation after the earthquake suggests that the failure mechanism of columns is affected by the existence of flare.

To understand the failure behavior of flared columns;

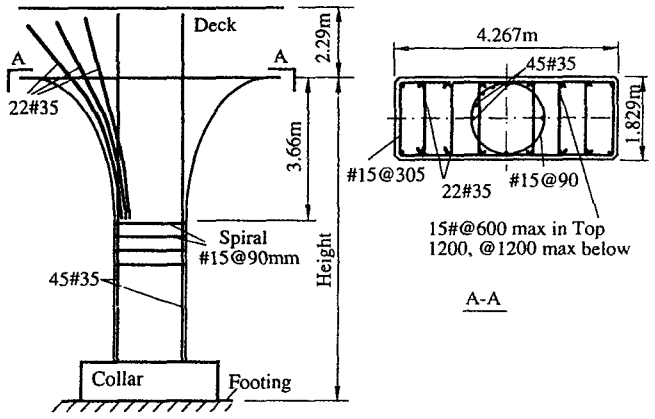

(a)

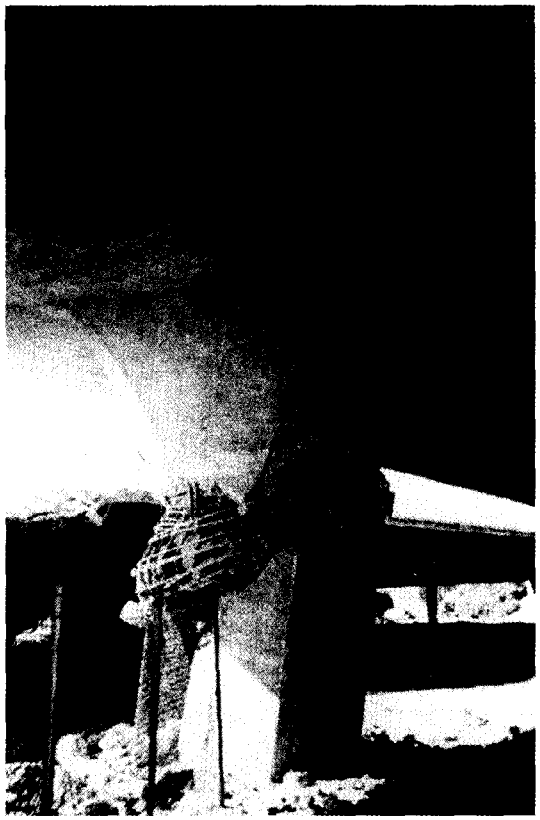

(b)

Fig. 2. Column of Mission-Gothic Undercrossing (a) details of reinforcement in column, (b) view of column damage.

nonlinear finite element analysis is used to study such a column under axial and lateral loads. Ottosens concrete failure criterion and constitutive model to determine secant modulus is incorporated into a nonlinear finite element model (Cheng and Lou, 1995). Isoparametric hexahedral elements with eight nodes are used for concrete, while reinforcement is modeled as elastoplastic material and uniformly distributed over concrete elements. Perfect bond

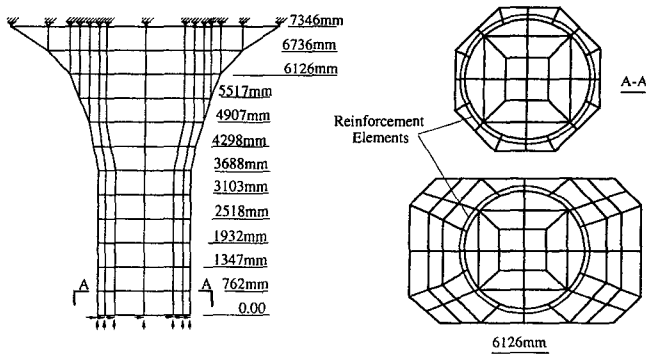

Fig. 3. Layout of finite element mesh for column R4L of Mission-Gothic Undercrossing.

between reinforcement and concrete is assumed before concrete cracks. But a smeared cracking model, as soon as concrete cracks, is applied to deal with the subsequent behavior of concrete. An algorithm of nonlinear analysis of reinforced concrete structures (NARCS) is developed for UNIX system (Lou and Cheng, 1994). The reliability of computer programs was demonstrated by huge computational efforts with comparison of vast experimental results (Lou, 1997; Lou and Cheng, 1996).

Fig. 3 shows the layout of finite element mesh for bridge column R4L. It is divided into 552 concrete elements and 312 reinforcement elements. Relative lateral displacement can be measured assuming there is no movement at the top of the column. Lateral force is equivalently applied at the bottom of column; dead load is 13,148 kN, uniformly distributed over nodes at the column's bottom surface. Compressive strength of concrete is 31.66 N/mm^2, measured by Caltrans from post-earthquake field test of the collapsed bridge structure. Yielding strength is 455 N/mm^2 for main column reinforcement, and 303 N/mm^2 for stirrup or spiral.

3.2 Interpretation of analytical results

Post-earthquake observation indicates that the bridge collapse was mainly caused by transverse ground motion. Thus two loading cases are selected to study the failure behavior of flared columns. One is the flared column subjected to lateral load along the strong axis of flares cross-section; the other is under lateral load at a 45° angle to the strong axis of flare. Dead load is considered in both cases. Note that these two loading cases represent columns of the right bridge structure at bent 4 and bent 2 or 3 under lateral load, respectively.

For the first case that column is under lateral load along the strong axis of the flare, the increment of lateral displacement is proportional to the increment of lateral force at the beginning of loading. When lateral load increases to

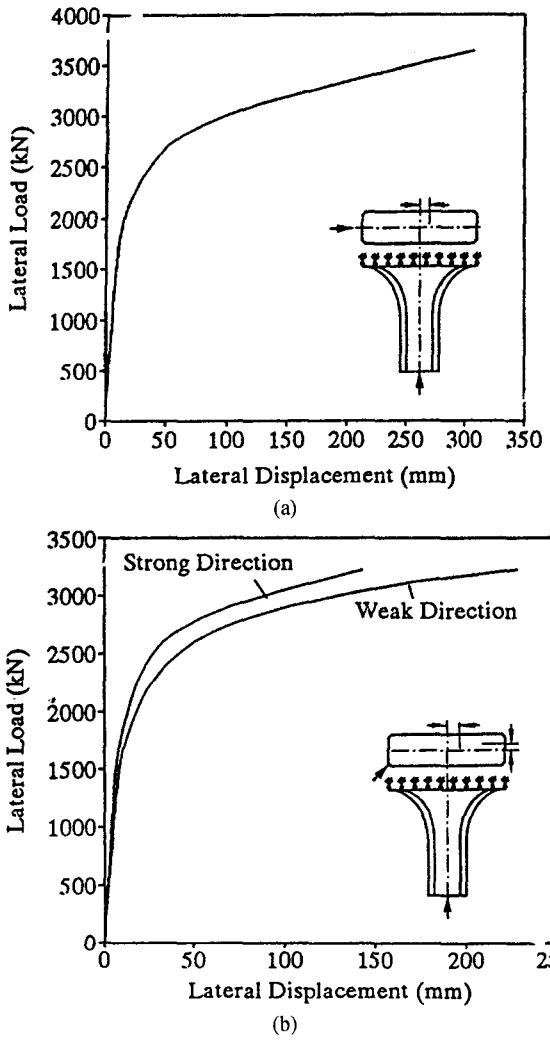

Fig. 4. Relation of load and displacement under lateral load (a) lateral load along strong axis, (b) lateral load at 45° to strong axis.

1,352 kN and corresponding displacement is 7.61 mm, cracks appear at the bottom of the flare and are perpendicular to the direction of lateral loading. Fig. 4a shows the relationship of lateral load and corresponding displacement. Due to large column cross-section and sufficient longitudinal reinforcement, the reduction of lateral stiffness just after concrete cracks is insignificant compared to uncracked column stiffness. Thus the relationship of load and displacement remains approximately linear after the appearance of cracks in small amounts. However, as lateral load increases, cracks increase and propagate. A decrease in stiffness is responsible for deviation of the load displacement curve. Consequently, nonlinear behavior of the column is clearly observed from the relationship of load and displacement. Longitudinal reinforcement begins to yield at lateral load of 2,288 kN (Fig. 4a). Fig. 5 shows a crack pattern, indicating that cracks develop mainly in the

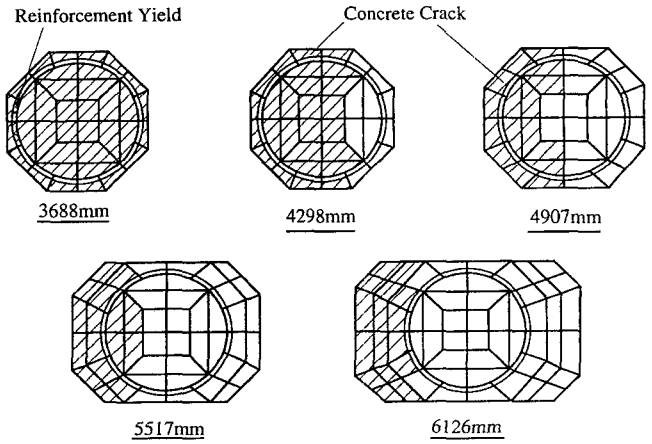

Fig. 5. Crack pattern of column under lateral load in strong axis.

flare's lower part. Columns in this region deform more easily. Ultimate load reaches 3,640 kN with lateral displacement of 308 mm. Failure mechanism depicted above are similar to column failure seen in post-earthquake field observation, which shows that concrete cracks and spiral rupture in the lower part of the flare led to column collapse in bent 4.

For columns subjected to lateral load at a 45° angle to the strong axis of the flares cross-section, load displacement curves at strong and weak axes are shown in Fig. 4b. These curves are similar to the curve of the first case. Cracks appear in the lower part of the flare first, and are perpendicular to the applied load. In other words, cracks have a 45° angle to the strong axis. Cracking load is 1,144 kN with displacement of 4.56 mm along the strong axis and 6.01 mm along the weak axis. Cracking load is lower than that of the first case. Load displacement curves in Fig. 4b indicate that under the same load, smaller displacement is observed in the strong than in the weak axis because the column in the flare region is much stiffer in the former. Column failure finally occurs in the weak axis plane. Ultimate load is 3,224 kN with a sudden increase of displacement from 174 mm to 229 mm along the weak axis. Concrete cracks appear mainly in the region of the flare. Field observation shows that damage began at the bottom of the flare where longitudinal reinforcement was not enclosed by stirrups; concrete cracks developed upward with spalling of concrete over the region of the flare (Priestley *et al.*, 1994). Nonlinear finite analysis reveals similar failure mechanism. Note that the ultimate load is about 13% lower than that of the first solution.

As indicated by this analysis, flare in the upper part of columns plays a role in column failure mechanism. If lateral load is applied along the strong axis of flare, column capacity increases due to the effect of flare. This effect on column capacity decreases with lateral load acting at a 45°

angle from the strong axis. Thus the unusual layout of skew bents unintentionally results in different column capacities.

4. Nonlinear Time-history Analysis of Bridge Collapse

4.1 Bridge Structural Model

Analysis of collapse behavior focuses on the right bridge structure. Though the left one suffered severe damage, columns displayed the same failure mechanism as those of the right bridge. The investigation of right bridge behavior can thus present the left one. A three-dimensional lumped mass model is depicted in Fig. 6. The bridge superstructure is considered as linear elements, and columns are modeled as nonlinear ones. This is because that the stiffness of superstructure is much greater than that of columns, and only column failure are expected. The collapse of superstructure resulted from column failure. Due to heavy flare, the upper part of the flare region is evenly divided into three elements, and equivalent cross-section is introduced to treat each columns segment as a straight-line element. The straight part of the column is modeled as a single element.

Elastic stiffness of each bearing pad is 3,200 kN/m using shear modulus G = 1.171 MPa, thickness of 76 mm, and 457 mm × 457 mm of bearing pad area (Cheng and Lou, 1996). Shear keys are used to restrain transverse movement at abutments. Columns are assumed to connect footings with hinges. Interaction between soil and foundation is not considered due to scant damage information.

A computer program ("IAI-NEABS" 1993) is employed to perform nonlinear time-history analysis. Column yielding surface, as a part of input file, is determined by BIAX computer program (Wallace, 1992). Detailed description of properties of superstructure and column segment, along with other parameters is reported elsewhere (Lou and Cheng, 1996).

Note that full length of abutment is used in the bridge model with the given skew angle. The connection between the superstructure and abutment is linked with springs. For convenient description, actual abutments at bridge's both ends are not shown in Fig. 6.

4.2 Ground Motion Modification

Seismic loading used herein for time-history analysis was recorded at Sylmar County Hospital parking lot, approximately 18 km from the epicenter. This recording station provided three-dimensional acceleration, velocity, and displacement at a time interval of 0.02 s. Peak ground acceleration was 0.604 g at 4.08 s in the east-west direction, 0.843 g at 4.20 s in the north-south direction, and 0.535 g at 3.96 s in vertical direction.

Due to lack of seismic instrumentation at the bridge, ground accelerations recorded at Sylmar County Hospital parking lot need to be modified for bridge analysis. The following peak-horizontal-acceleration attenuation equation is adopted to modify acceleration a' at Mission-Gothic Undercrossing (Campbell, 1981).

$$a' = a\left(\frac{R_2 + 0.0606e^{0.7M}}{R_1 + 0.0606e^{0.7M}}\right)^{1.09} \quad (1)$$

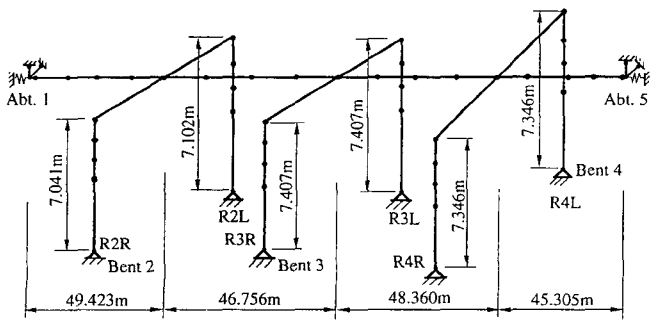

Fig. 6. Lumped mass model for right bridge structure of Mission-Gothic Undercrossing.

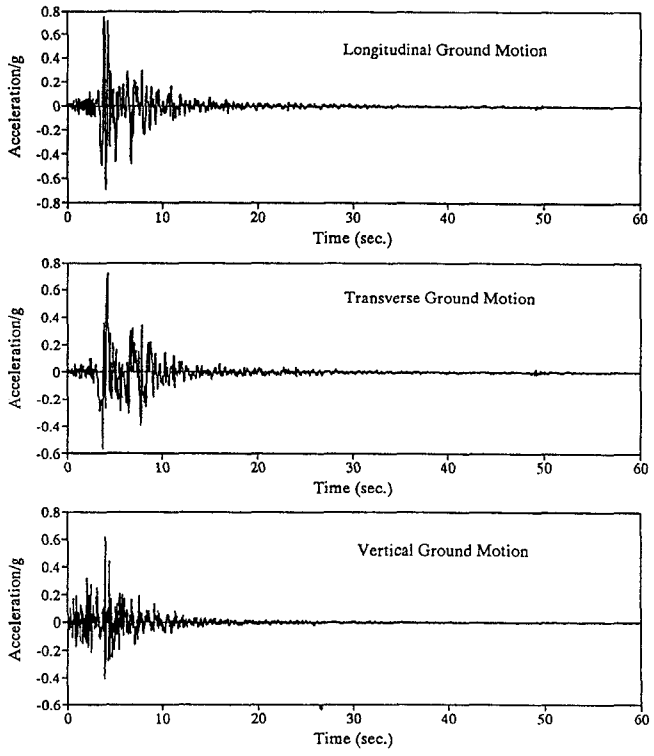

Fig. 7. Modified accelerations in longitudinal, transverse and vertical directions.

Where a = peak acceleration in g at Sylmar County Hospital parking lot, M = magnitude of earthquake (6.7), R_1, R_2 = distance from epicenter to Mission-Gothic Undercrossing (7.5 km) and Sylmar County Hospital parking lot (18 km), respectively. Thus the modifying coefficient is $a'/a = 1.16$ for all components. Accelerations in east-west and north-south direction are also modified to be consistent with longitudinal and transverse directions of the right bridge structure. Fig. 7 shows modified accelerations in longitudinal, transverse and vertical directions.

4.3 Dynamic analysis of Bridge Structure

Four types of different directional ground motion are chosen as seismic input for nonlinear time-history analysis to determine the dominant directional effects of ground motion on structure collapse. They are 1) longitudinal, 2) transverse, 3) longitudinal and transverse, and 4) longitudinal, transverse and vertical, or three-dimensional ground motion. Analysis is performed by IAI-NEABS ("IAI-NEABS" 1993).

The right structure was partially damaged under longitudinal ground motion. Column R3L first yields in the flare's lower part at 4.04 s. After 0.02 s, columns R2R, R2L, and R3R also yield in the flare's lower part. Yield does not develop elsewhere in these columns, and columns at bent 4 do not yield. Therefore, the bridge structure will not collapse if the dominant movement of the earthquake is in the bridge's longitudinal direction. Under transverse ground motion, the lower part of columns R3R and R3L first yields at 3.38 s. Corresponding transverse displacement at column R3R is 31 mm. Maximum transverse displacement of 75 mm is observed at 8.38 s. Columns R4L and R4R yield at 3.44 s and 3.98 s, respectively. Yielding extends to the upper part of each column and failure of all columns occurs. Thus the collapse of the bridge is mainly caused by transverse ground motion. For the case of the bridge structure under longitudinal and transverse ground motion, analytical results show that longitudinal displacement greatly increases. The added factor of dual directional ground motion leads to an increase of internal forces in columns. But transverse ground motion is still a dominant cause of the bridge collapse (Cheng and Lou, 1996).

To obtain more detailed knowledge of the bridges collapse behavior, the right structure is analyzed under longitudinal, transverse, and vertical ground motion. Fig. 8 summarizes column's yielding situation of the right structure under three-dimensional ground motion. This structure yields at columns R3R and R3L in the flares lower part at 3.38 s. After 0.06 s, columns R4R and R4L then yield. Columns R2L and R2R yield at 3.40 s and 3.48 s, respectively. All columns first yield in the lower part of the flare. Columns at bent 3 fail severely, while columns at bent 2 and 4 sustain damage in the middle or lower part of the flare. Failure of columns results in collapse of the bridge's superstructure. The yielding pattern shown in Fig. 8 gives a view of bridge collapse behavior similar to that observed in the field. All columns yield within 0.7 s after 3.38 s. This suggests that the bridge collapses in a sudden manner.

Failure of shear keys at abutment 1 and 5 can be considered as a shear-friction problem and evaluated using the equation of ACI 318R-89, R11.7.3 ("Building" 1992).

$$V_n = 0.8A_{vf}f_y + A_cK_l \tag{2}$$

where V_n = shear strength; A_{vf} = area of shear-friction reinforcement, in.^{2}; f_y = yield strength of shear-friction reinforcement, psi; A_c = area of concrete section resisting shear

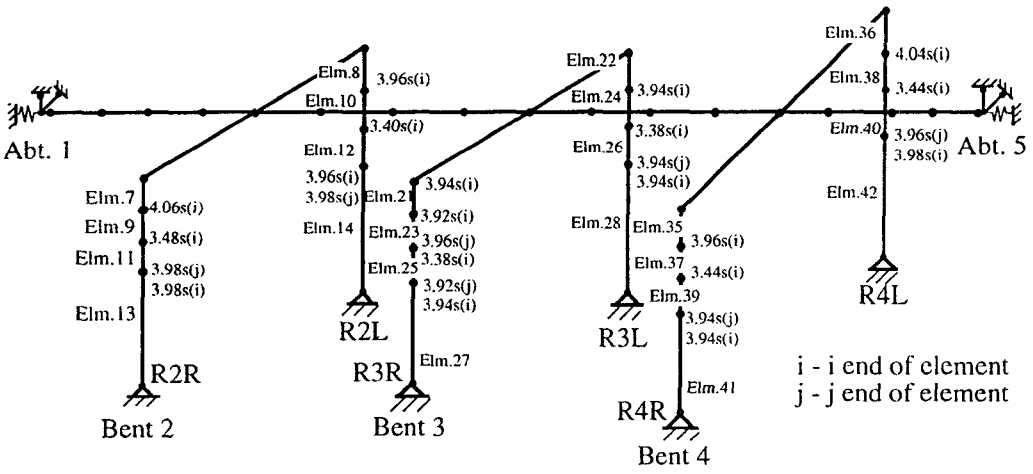

Fig. 8. Yielding pattern of right bridge structure due to 3d seismic input of Mission-Gothic Undercrossing.

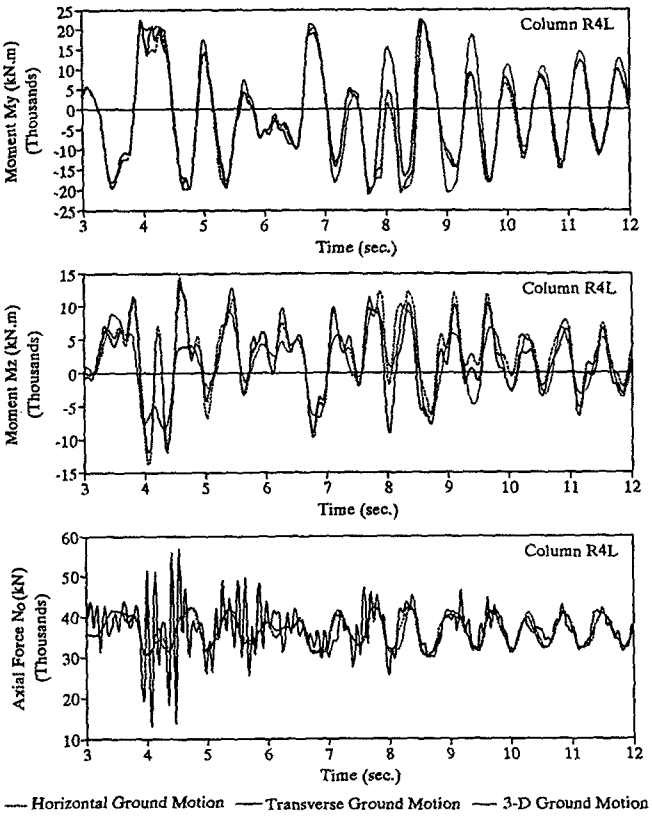

Fig. 9. Comparison of M_y, M_z and N at R4L of Mission-Gothic Undercrossing.

transfer, in.^{2}; and $K_1 = 400$ psi for normal weight concrete. V_n can be multiplied by a coefficient of 4.45 and transferred into shear strength in SI unit (N). Shear-friction reinforcement of each shear key is 16#15 and $A_{vf} = 3{,}200$ mm^2 (4.96 in.^{2}). $f_y = 414$ MPa (60,000 psi). $A_c = 580{,}644$ mm^2 (900 in.^{2}). Shear strength of three shear keys at each abutment is 7,984 kN (1,794 kips), much less than maximum shear forces of 47,393 kN (4.32 s) at abutment 1 and 36,535 kN (4.32 s) at abutment 5, respectively. Shear keys at both abutments are expected to fail at 3.3 s. compared with column yielding, shear keys fail prior to yielding of columns at bent 3. It suggests that bridge begins with rotation after the failure of shear keys. Since the time interval between shear keys failure and columns yielding is very small (0.08 s), bridge rotation is not expected to have great influence on initial yielding of columns. However, with the continuity of the earthquake, the bridge rotation generates torsional effects on columns and accelerates bridge collapse.

Fig. 9 presents a comparison of moment M_y (in strong axis), M_z (in weak axis) and axial force N_o at the bottom of the flare of column R4L (i-end of element 42). Difference in moments at the same time is observed due to different directional ground motion. At 4.58 s, moment M_z caused by three-dimensional ground motion is 14,513 kN-m. But M_z caused by transverse ground motion is only 3,803 kN-m. The former is approximately 3.8 times the latter. At the same time, moment M_y (12,496 kN-m) under three-dimensional ground motion is greater than that (11,760 kN-m) caused by transverse ground motion. As shown in Fig. 9, the influence of vertical ground motion on a columns internal forces is apparent. Under three-dimensional ground motion, axial force N_o is 56,070 kN at 4.42 s, which is 68% greater than that (33,335 kN) under transverse ground motion. Therefore, consideration of vertical ground motion in time-history analysis can yield columns unfavorable internal forces.

4.4 Effect of Flare on Structural Performance

As mentioned above, the flare was not purposely designed to strengthen the bridge columns. But the failure mechanism of bridge columns implies that the existence of

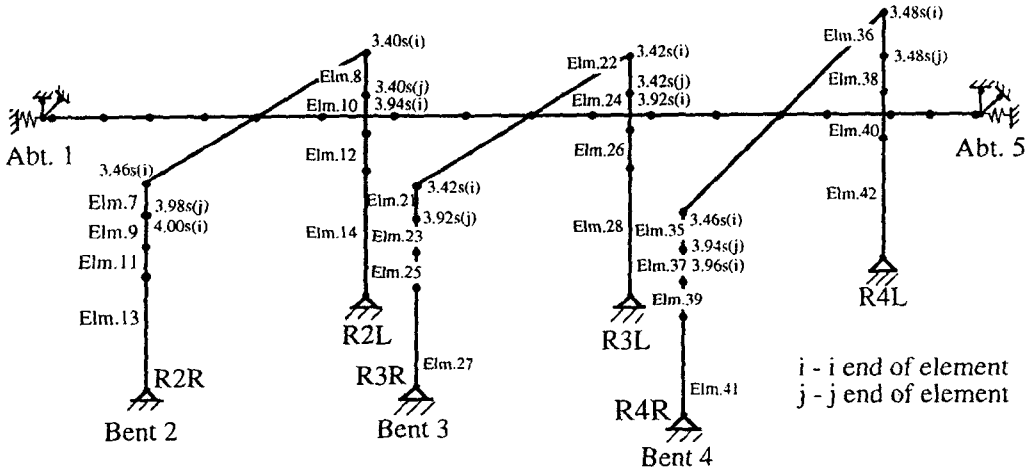

Fig. 10. Yielding pattern of structure without flare under 3D seismic input of Mission-Gothic Undercrossing.

flare changes the damage pattern of a column. A three-dimensional structural model, identical to that in Fig. 6 except for the absence of flare in the upper part of columns, is used here to investigate the influence of flare on structural performance under the three components of ground motion.

Fig. 10 shows the yielding pattern of the right structure with no flare in the upper part of columns. Yielding begins at the top of column R2L (3.40 s); then columns R3L and R3R yield at their upper ends after 0.02 s. At 3.46 s, columns R2R and R4R yield. Column R4R reaches yielding at 3.48 s. All columns enter yielding stages from the top, and yielding extends toward the middle part of columns. This yielding pattern is totally different from that with flare in the upper part of columns. This numerical solution indicates that the effect of flare cannot be neglected in predicting bridge failure mechanism. Fig. 11 compares transverse displacement at column R3L with and without flare; peak transverse displacement is less with than without it. This is because flare increases stiffness in the upper part of columns.

A question of comparable seismic resistance is raised by the effect of the flare on bridge structural performance. Note that the volume of flare at each column is approximately 6.116 m^3 while the volume of the column itself is approximately 19.831 m^3. Thus the use of flare augments about 31% of column mass. Under ground motion, the increase of structural mass is known to lead to an enlargement of external response. Corresponding internal force also becomes larger before column yields. Due to the existence of flare and little increase in its strength, a bridge structure with flared columns has less seismic resistance, and is more likely to suffer damage or collapse. Such a bridge structure reaches yield earlier than one without flare. Therefore, the use of flare is not recommended because it may have an unfavorable effect on bridge performance. If it has to be used for aesthetic reasons, circular flare is recommended so that column capacity is independent of skew bents. Supplementary spiral is also needed in the lower part of the flare to enclose flare reinforcement and prevent propagation of concrete spalling.

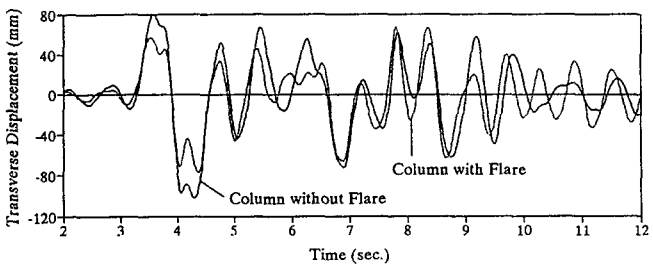

Fig. 11. Comparison of transverse displacement of column R3L of Mission-Gothic Undercrossing.

5. Summary

Significant conclusions applicable to professional design, based on post-earthquake assessment, are summarized as follows.

1. Mission-Gothic Undercrossing collapsed due to these factors: a) skews of bents and abutments; b) directional dependence of flared column stiffness; and c) lack of stirrups in the lower part of the flare to enclose flare reinforcement. After shear keys fail, torsional effects due to skew bents and abutments will accelerate the bridge collapse. The skew layout of column flare produces different stiffness of columns and column capacities in transverse or longitudinal direction so that different failure mechanism of columns are observed.

2. Nonlinear finite element analysis indicates that column failure mechanism is entirely affected by the column's flare. Column capacity depends on the angle of lateral force to the strong axis of flared column cross-section. A 13% reduction of column capacity is observed due to the skew of a 45° angle from the strong axis of a flared column cross-section.

3. Structural analyses under different directional ground motion show that transverse ground motion is the dominant cause of bridge collapse. Three-dimensional ground motion results in a more accurate description of bridge collapse. Inclusion of vertical ground motion in time-history analysis can cause column's unfavorable internal forces. Collapse behavior based on numerical solutions is similar to that observed in the field after the earthquake.

4. Time-history analysis also shows that flare plays an important role in a bridge column failure mechanism. The existence of flare increases column mass and internal force in columns, and changes the location of plastic hinges from the top of columns to the middle. Moreover, a structure with flare reaches yielding stage earlier than one without it.

5. Use of flare in the upper part of columns is not recommended. If flare has to be used for aesthetic reasons, circular flare is suggested so that uniform column stiffness is expected and column capacity has no dependence on skew bent. Supplementary spiral is needed in the flare's lower part to enclose flare reinforcement and prevent propagation of concrete spalling.

Acknowledgment

This project is supported by National Science Foundation under Grant No. NSF CMS 6416463, as well as MRTC and ISC at UMR. D.W. Liu, principal with Imbsen & Associates Inc. and L.H. Sheng senior engineer at Dept. of Transportation, Sacramento, Calif. provided technical advice and cooperation. The support and assistance are gratefully acknowledged.

References

American Concrete Institute (1992) Building code requirements for reinforced concrete and Commentary ACI 318-89/ACI 318R-89, American Concrete Institute (ACI), Detroit, Mich.

Campbell KW (1981) Near-source attenuation of peak horizontal acceleration, Bulletin of the Seismological Society of America, 71(6): 2039-2070.

Cheng FY, Lou KY (1997) Collapse studies of Mission-Gothic Undercrossing and Bull Creek Canyon channel bridge during the January 17, 1994 Northridge earthquake, NSF, Final rep., US Dept. of Commerce, NTIS, Accession No. PB97-117881.

Cheng FY, Lou KY (1996) Assessment of a bridge collapse and its design parameters for Northridge earthquake, Post-earthquake rehabilitation and reconstruction, Elsevier Science Ltd., F.Y. Cheng and Y. Wong, eds.: 7-20.

Cheng FY, Lou KY (1995) Inelastic behavior and load displacement equations of low-rise RC solid and perforated shear walls, Urban disaster mitigation: the role of engineering and technology, Elsevier Science Ltd., F.Y. Cheng and M.S. Sheu, eds.: 79-96.

Cheng FY, Lou KY, Yang JS (1994) Analytical and experimental studies of RC structures with low-rise shear walls, Proc., 5th U.S. Natl. Conf. On Earthquake Engrg., Chicago, Ill.., 1: 45-54.

IAI-NEABS user manual (1993) Imbsen & Associates Inc., Sacramento, Calif.

Imbsen RA, Penzien J (1984) Evaluation of energy absorption characteristics of highway bridges under seismic conditions, 1 and 2, rep. UCB/EERC-84/17, Earthquake Engineering Research Center, University of California at Berkeley, Berkeley, Calif.

Lou KY (1997) 3-D nonlinear finite element analysis of reinforced concrete low-rise wall structures and bridges under earthquake excitations, Ph.D. dissertation, Dept. of Civil Engineering, Univ. of Missouri-Rolla, Rolla, Mo.

Lou KY, Cheng FY (1994) NARCS: A computer program for nonlinear analysis of reinforced concrete structures, Department of Civil Engineering, University of Missouri-Rolla, Rolla, Mo.

Lou KY, Cheng FY (1996) Post-earthquake assessment of bridge collapse and design parameters, 11 World Conference on earthquake engineering, Acapulco, Mexico.

NCEER (1994) The Northridge, California earthquake of January 17, 1994: Performance of highway bridges Rep. NCEER-94-0008, National Center for Earthquake Engineering Research, State University of New York at Buffalo, Buffalo, N.Y., I.G. Buckle, ed.

EERC (1994) Preliminary report on the seismological and engineering aspects of the January 17, 1994 Northridge earthquake Rep. UCB/EERC-94/01, Earthquake Engineering Research Center, University of California at Berkeley, Berkeley, Calif. J.P. Moehle, ed.

Priestley MJ, Seible F, Uang CM (1994) The Northridge earthquake of January 17, 1994: Damage analysis of selected freeway bridges, Rep. SSRP-94/06, Department of Applied Mechanics and Engineering Sciences, University of California at San Diego, San Diego, Calif.

Wallace JW (1992) BIAX: A computer program for the analysis of reinforced concrete and reinforced masonry sections, Rep. CU/CEE-92/4, Department of Civil Engineering, Clarkson University, Potsdam, N.Y.

Appendix I. Notations

The following symbols are used in this paper:

A_c = area of concrete section resisting shear transfer, in.^{2}
A_{vf} = area of shear-friction reinforcement, in^2
a = peak acceleration at record station
a' = modified acceleration at studied bridges
f'_c = compressive strength of concrete, MP
f_y = yield strength of shear-friction reinforcement, psi or MP
K_1 = coefficient for different concrete
R_1, R_2 = distance from the epicenter to studied bridges and record station, respectively, km
M = magnitude of earthquake
M_y, M_z = moment capacity of two principal axes of member cross-section, kN-m
N_o = compressive axial force, N
P_o = compression capacity, kN
V_n = shear strength of shear key